ChemComm

This article is part of the

Chirality
web themed issue

Guest editors: David Amabilino and Eiji Yashima

All articles in this issue will be gathered together online at

www.rsc.org/chiral

ChemComm

Dynamic Article Links

Cite this: *Chem. Commun.*, 2012, **48**, 3665–3667

www.rsc.org/chemcomm

COMMUNICATION

Helical phase from blending of chiral block copolymer and homopolymer

Hsiao-Fang Wang,[a] Hsin-Wei Wang[a] and Rong-Ming Ho*[ab]

Received 30th December 2011, Accepted 15th February 2012
DOI: 10.1039/c2cc18163k

The phase behavior of the binary blends of polystyrene-*b*-poly(L-lactide) chiral block copolymer (BCP*) and polystyrene homopolymer (HS) is found to be strongly dependent on the molecular weight (M_n) of the HS. A helical phase is formed in the blends with low-M_n HS due to an enhancement of helical steric hindrance.

Self-assembly is the spontaneous organization of components into patterns or structures by cooperating secondary interactions (*i.e.*, non-covalent bonding forces).[1,2] Nature uses the self-assembly of molecules and supramolecules for structuring substances so as to form various biological architectures.[3] Of them, helical morphology is perhaps the most fascinating morphology in nature. The chirality of compounds has been identified as one of the main origins of the formation of helical textures.[4–7] Block copolymers (BCPs) are able to self-assemble into periodic nanostructures in bulk because of the incompatibility and the chemical connection between constituent blocks.[8–11] Hierarchical superstructures with a helical sense can be obtained by self-assembling amphiphilic BCPs containing a charged chiral block in solution, suggesting that the effect of chirality might play an important role in the formation of helical nanostructures.[12] Recently, block copolymers composed of chiral blocks (denoted chiral block copolymers (BCPs*)), such as poly(styrene)-*b*-poly(L-lactide)s (PS-PLLA)s, have been designed for self-assembly.[13–15] Twisted textures under transmission electron microscopy (TEM) projection can be observed in the bulk samples of the PS-PLLA, whereas no such projection image in racemic BCPs (poly(styrene)-*b*-poly(D,L-lactide) (PS-PLA)) can be found, suggesting the chirality effect on BCP self-assembly.[13] Consequently, a helical phase possessing hexagonally packed PLLA helical nanostructures in a PS matrix is identified as a new phase with the space group of *P*622.[15]

A hypothetical mechanism for the formation of the helical phase is proposed.[15] Owing to the effect of chirality (the helical steric hindrance) on molecular packing and microdomain stacking, each microphase-separated domain will twist and shift toward the others during morphological evolution from self-assembly, yielding the helical curvature at the interface, and giving a helical nanostructure to develop. Namely, the formation of helical microdomains in the PS-PLLA is initiated from the microphase-separated interface, and then amplified by the incompatible PS block. Blending homopolymer into BCP can obviously enrich the phase behavior of the BCP. For the blends of BCP with a selective homopolymer, *i.e.*, compatible with one of the constituent blocks in the BCP, the phase behavior for the binary blends depends strongly on the compatibility resulting from the affinity of the homopolymer with the constituent blocks and the corresponding molecular weight (M_n) of the homopolymer to that of the selected block in the BCP.[16–18] In this study, we aim to investigate the feasibility of forming helical phase by blending PS homopolymers (HS) with different M_ns into the PS-PLLA for self-assembly so as to examine the suggested mechanism for the formation of the helical microdomains initiating from the microphase-separation interface. The chemical structures of PS-PLLA and HS are illustrated in Scheme 1.

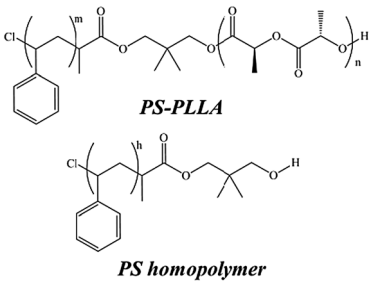

Scheme 1 Chemical structures of PS-PLLA BCP* and PS homopolymer.

On the basis of the phase behavior of the PS-PLLAs,[15] a PS-PLLA with a lamellar phase (symmetric composition) was used for the preparation of the binary blends so as to bring the expected compositions for the formation of the helical phase from blending. The binary blends were prepared by solution casting followed by rapid cooling from the microphase-separated melt at 175 °C at the cooling rate of 150 °C min^{-1} to 25 °C. Consequently, amorphous microphase-separated phase can be formed without the effect of the PLLA crystallization on the self-assembled morphology. The PS-PLLA with PLLA volume fraction (f^v_{PLLA}) of 0.48, exhibiting lamellar phase, was used for blending. The f^v_{PLLA} in the blends was 0.33 for all of the blends examined in this study. Fig. 1(a) shows the TEM micrograph for the blends of PS-PLLA with high-M_n HS (M_n = 39 000 g mol^{-1}). RuO_4-stained PS microdomains appear as dark regions, whereas polylactide microdomains appear as bright regions, suggesting the preservation of lamellar phase (namely, there is no occurrence of phase transformation). The corresponding 1D SAXS profile

[a] *Department of Chemical Engineering, National Tsing Hua University, Hsinchu, 30013, Taiwan, R.O.C. E-mail: rmho@mx.nthu.edu.tw; Fax: +886-3-5715408; Tel: +886-3-5738349*
[b] *Frontier Research Center on Fundamental and Applied Sciences of Matters, National Tsing Hua University, Hsinchu, 30013, Taiwan, R.O.C.*

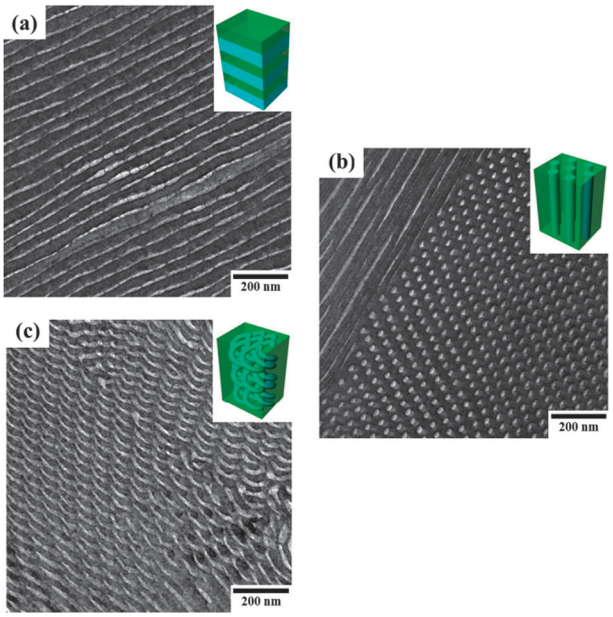

Fig. 1 TEM micrographs for the blends of PS-PLLA with high-M_n HS (M_n = 39 000 g mol^{-1}) (a), intermediate-M_n HS (M_n = 13 400 g mol^{-1}) (b), and low-Mn HS (M_n = 3000 g mol^{-1}) (c).

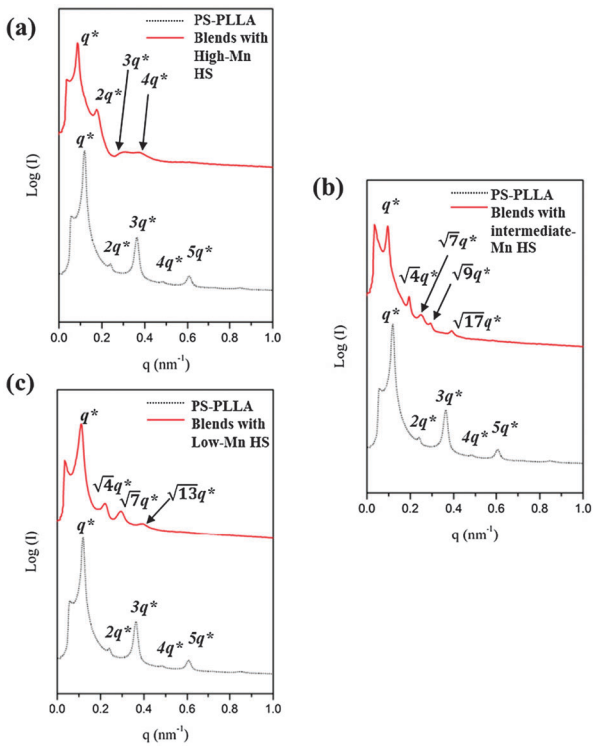

Fig. 2 1D SAXS profiles for the blends of PS-PLLA with high-M_n HS (M_n = 39 000 g mol^{-1}) (a), intermediate-M_n HS (M_n = 13 400 g mol^{-1}) (b), and low-M_n HS (M_n = 3000 g mol^{-1}) (c).

(Fig. 2(a)) shows reflections at q^* ratios of 1 : 2 : 3 : 4, further demonstrating the preservation of lamellar phase. Moreover, no macrophase separation is observed under TEM, and significant shifting of reflection peaks to lower q in the SAXS result is found, suggesting that the introduction of the HS should be localized in between the PS blocks (as illustrated in Fig. 3(b))

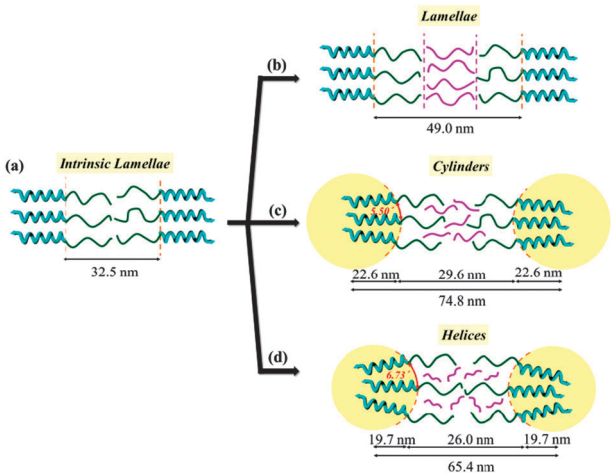

Fig. 3 Illustration of (a) the intrinsic lamellae of PS-PLLA, and the molecular dispositions for the blends of PS-PLLA with (b) high-M_n HS, (c) intermediate-M_n HS, and (d) low-M_n HS. The sizes of the PS microdomain and the PLLA microdomain are determined based on the primary peaks of the SAXS profiles. Fig. 3(c) and (d) show the calculation results of the radian between two chemical junctions in the PLLA microdomain (r_{PLLA}) as indicated by the red arc line. r_{PLLA} is approximately 6.73° in helical phase, and 5.50° in cylindrical phase.

so as to enlarge the size of the PS microdomains from 32.5 to 49.0 nm, as determined from the primary peaks of the SAXS profiles. Fig. 1(b) shows the TEM micrograph for the blends of the PS-PLLA with intermediate-M_n HS (M_n = 13 400 g mol^{-1}). Hexagonally packed cylinders can be identified under TEM observation. Also, the hexagonally packed cylindrical phase can be clearly identified by the corresponding 1D SAXS profile (Fig. 2(b)) in which the reflections occur at q^* ratios of $1 : \sqrt{4} : \sqrt{7} : \sqrt{9} : \sqrt{17}$, inferring a phase transformation from lamellae to cylinders. We speculate that the phase transformation from lamellae to cylinders is driven by a solubilization of introducing HS, as illustrated in Fig. 3(c). The introduction of the HS gives rise to the swelling of the PS microdomains both laterally and longitudinally, resulting in an expansion of the average distance between chemical junctions and a change in microdomain size. Subsequently, the increase in the enthalpy penalty due to the incompatibility between the PLLA and PS polymer chains will be balanced by a reduction of interfacial area so as to result in the phase transformation from lamellae to cylinders.

Most interestingly, while the M_n of introduced HS is much lower than that of the PS block in the PS-PLLA, for instance M_n = 3000 g mol^{-1}, complicated projections under TEM can be obtained (Fig. 1(c)). Instead of cylindrical projection, twisted morphology can be found in the blends. The reflection peaks in the corresponding 1D SAXS profile occur at q^* ratios of $1 : \sqrt{4} : \sqrt{7} : \sqrt{13}$ (Fig. 2(c)), suggesting a hexagonally packed character. Notably, in contrast to the blends with intermediate-M_n HS, a helical phase instead of a cylindrical phase is found in the blends using low-M_n HS for blending. We speculate that the low-M_n HS can be homogeneously distributed into the PS microdomains of the PS-PLLA so as to give a higher tendency to allocate the HS near the microphase-separated interface than that in the blends with higher M_n. The phase behavior of the allocation of the HS near the interface is

Table 1 Characterization of blends of PS-PLLA with HS

	Morphology	D/ nm	R_{PLLA}/ nm	D_{PS}[a]/ nm	D_{PLLA}[b]/ nm
Blends with high-M_n HS	Lamellae	73.1	—	49.0	24.1
Blends with intermediate-M_n HS	Cylinder	74.8	22.6	—	—
Blends with low-M_n HS	Helix	65.4	19.7	—	—

[a] D_{PS} is the size of PS microdomain. [b] D_{PLLA} is the size of PLLA microdomain.

similar to the BCP composites with inorganic nanoparticles in which the nanoparticles with small size tend to aggregate near the microphase-separated interface on the basis of theoretical predictions.[19] Subsequently, the occurrence of the local segregation of the HS near the microphase-separated interface gives rise to significant helical steric hindrance for the formation of helical curvature through a twisting and shifting mechanism, and eventually helps develop a helical phase. We speculate that the behavior of the enhancement in the helical steric hindrance is similar to the morphological change by blending with a small concentration of compatible polymer diluents in which the effect of helical steric hindrance will be significantly enhanced by increasing the diluents fraction.[20,21] As a result, as illustrated in Fig. 3, the radian between two chemical junctions in the PLLA microdomains with helical phase should be larger than that in the blends with cylindrical phase.

To further examine the suggested hypothesis, systematic calculation is conducted on the basis of the SAXS results. By assuming that the number of PLLA chains comprising a microdomain is equal to the ratio of the microdomain volume (V_{domain}) to the molecular volume of a PLLA chain (v_{PLLA}), the radian between two chemical junctions in the PLLA microdomain can thus be determined.

$$\frac{V_{domain}}{v_{PLLA}} = \text{number of chains} = \frac{S_{domain}}{\sigma} \qquad (1)$$

S_{domain} is the microdomain surface area. σ is the area at the surface of microdomain occupied by a single PLLA chain, which can be replaced by $\sigma = 2v_{PLLA}/R_{PLLA}$ because the surface-to-volume ratio of microdomain for both cylinder and helix is $2/R_{PLLA}$,[22] where R_{PLLA} is the radius of the PLLA microdomain and can be determined by the following equation, $R_{PLLA} = \sqrt{\sqrt{3}f_{PLLA}^{v}/2\pi D}$. D is the interplanar spacing, determined by the primary peak of the SAXS profile. The calculated results are summarized in Table 1. Also, v_{PLLA} can be replaced by the equation $v_{PLLA} = M_{PLLA}/(\rho_B \times N_{Av})$, where M_{PLLA} is the molar mass of the PLLA chain, N_{Av} is Avogadro's number, and ρ_B is the density of the PLLA chain. For instance, in our blending system, M_{PLLA} is 39 600 g mol^{-1} and ρ_B is 1.248 g cm^{-3}. Accordingly, the calculated result of v_{PLLA} is 52.88 nm^3 and σ is 4.68 nm^2 for the cylindrical phase and 5.36 nm^2 for the helical phase. Furthermore, the number of PLLA chains within the microdomain (N) can be described as $N = (\pi \times R_{PLLA}^2 \times \sqrt{\sigma})/v_{PLLA}$.[16] As a result, the radian between two chemical junctions in the PLLA microdomain ($r_{PLLA} = 360^\circ/N$) in the helical phase (approximately 6.73°) is higher than the radian in the cylindrical phase (approximately 5.50°), implying that the low-M_n HS indeed tends to be allocated near the microphase-separated interface so as to enlarge the radian between two chemical junctions in the PLLA microdomain.

In summary, a helical phase can be formed by blending the PS-PLLA and the low-M_n HS, and examined by TEM and SAXS. The formation of helical phase is attributed to the enhancement of helical steric hindrance, resulting from the occurrence of the allocation of the low-M_n HS near the microphase-separated interface. Consequently, the mechanism of forming helical phase by blending BCP* and homopolymer may provide further understanding for the formation of the helical phase due to the chirality effect on BCP self-assembly.

We thank National Science Council of Taiwan (NSC 99-2120-M-007-003) for financial support.

Notes and references

1 J. M. Lehn, *Science*, 1985, **227**, 849–856.
2 G. M. Whitesides and B. Grzybowski, *Science*, 2002, **295**, 2418–2421.
3 G. A. Petsko and D. Ringe, *Protein Structure and Function, London*, New Science Press, London, 2004.
4 H.-S. Kitzerow and C. Bahr, *Chirality in Liquid Crystals*, Springer Press, New York, 2001.
5 J. J. L. M. Cornelissen, A. E. Rowan, R. J. M. Nolte and N. A. J. M. Sommerdijk, *Chem. Rev.*, 2001, **101**, 4039–4070.
6 M. M. Green, R. J. M. Nolte and E. W. Meijer, *Materials-Chirality, vol. 24 of Topics in Stereochemistry*, ed. S. E. Denmark and J. Siegel, Wiley, Hoboken, NJ, 2003.
7 R.-M. Ho, Y.-W. Chiang, S.-C. Lin and C.-K. Chen, *Prog. Polym. Sci.*, 2011, **36**, 376–453.
8 E. L. Thomas, D. M. Anderson, C. S. Henkee and D. Hoffman, *Nature*, 1988, **334**, 598–601.
9 F. S. Bates and G. H. Fredrickson, *Annu. Rev. Phys. Chem.*, 1990, **41**, 525–557.
10 J. T. Chen, E. L. Thomas, C. K. Ober and G.-P. Mao, *Science*, 1996, **273**, 343–346.
11 F. S. Bates and G. H. Fredrickson, *Phys. Today*, 1999, **52**, 32–38.
12 J. J. L. M. Cornelissen, M. Fischer, N. A. J. M. Sommerdijk and R. J. M. Nolte, *Science*, 1998, **280**, 1427–1430.
13 R.-M. Ho, Y.-W. Chiang, C.-C. Tsai, C.-C. Lin, B.-T. Ko and B.-H. Huang, *J. Am. Chem. Soc.*, 2004, **126**, 2704–2705.
14 R.-M. Ho, C.-K. Chen and Y.-W. Chiang, *Adv. Mater.*, 2006, **18**, 2355–2358.
15 R.-M. Ho, Y.-W. Chiang, C.-K. Chen, H.-W. Wang, H. Hasegawa, S. Akasaka, E. L. Thomas, C. Burger and B. S. Hsiao, *J. Am. Chem. Soc.*, 2009, **131**, 18533–18542.
16 H. Tanaka, H. Hasegawa and T. Hashimoto, *Macromolecules*, 1990, **23**, 4378–4386.
17 H. Tanaka, H. Hasegawa and T. Hashimoto, *Macromolecules*, 1991, **24**, 240–251.
18 H. Tanaka, H. Hasegawa and T. Hashimoto, *Macromolecules*, 1994, **27**, 6532–6540.
19 R. B. Thompson, V. V. Ginzburg, M. W. Matsen and A. C. Balazs, *Science*, 2001, **292**, 2469–2472.
20 H. D. Keith, F. J. Padden, Jr. and T. P. Russell, *Macromolecules*, 1989, **22**, 666–675.
21 C. C. Chao, C. K. Chen, Y. W. Chiang and R. M. Ho, *Macromolecules*, 2008, **41**, 3949–3956.
22 O. Tcherkasskaya, S. Ni and M. A. Winnik, *Macromolecules*, 1996, **29**, 4241–4246.